arXiv:cond-mat/0212510v1 [cond-mat.supr-con] 20 Dec 2002

Peak-effect and surface crystal-glass transition for surface-pinned vortex array

B. Plaçais, N. Lütke-Entrup, J. Bellessa, P. Mathieu, Y. Simon, and E.B. Sonin[1]

Laboratoire de Physique de la Matière Condensée de l'Ecole Normale Supérieure,

CNRS-UMR8551, 24 rue Lhomond, 75231 Paris, France

[1]*Racah Institute of Physics, Hebrew University of Jerusalem, Jerusalem 91904, Israel*

(February 1, 2008)

Abstract

The peak effect has been investigated in clean Nb crystals with artificially corrugated surfaces by measuring the linear surface impedance in the 1kHz-1MHz frequency range. From a two-mode analysis of the complex spectra, we establish that vortex dynamics is governed by surface pinning and deduce the associated vortex slippage length. We demonstrate experimentally and theoretically that the peak effect is related to a transition from collective to individual surface pinning. A proper account of the peak-effect anomalies implies softening of the shear rigidity by disorder-induced lattice deformations. This leads to a vortex crystal-glass transition induced by surface defects.

PACS numbers: 74.60.Ge

Typeset using REVTEX

The peak effect (PE) is a well known anomaly of the mixed state due to vortex lattice (VL) softening in the presence of random defects [1,2]. It is observed at the upper critical field B_{c2} of clean superconductors [3,4], well below B_{c2} in disordered oxide superconductors (second peak), or at the vortex-melting line in very clean $YBa_2Cu_3O_7$ crystals [5]. The physics of PE is the *order-disorder transition*, which is of interest for a broad range of elastic media. Recent developments concern vortices in conventional materials (Nb, $NbSe_2$), where PE is investigated in great detail [6–8]. Originally believed to be a crossover from collective to individual vortex pinning according to the Larkin-Ovchinnikov (LO) scenario [2], PE is now considered as a genuine transition [6,8], with a quasi-long-range order (Bragg-Glass) in the low-field phase [9,10]. However, strong limitations for a quantitative analysis of the phenomenon arise from the poor knowledge about the random defects responsible for PE.

In this work we consider a new situation where this difficulty can be overcome : the peak effect due to the *surface pinning of vortices*. The pinning landscape is provided by the surface corrugation $\zeta(\mathbf{r})$ of a slab in perpendicular or tilted magnetic field; a controlled roughness $\zeta^* \sim$ 1-10nm is produced by ion beam etching (IBE) and measured by atomic-force microscopy (AFM). Far from the upper critical field B_{c2} the intervortex interaction is strong and suppresses the surface pinning. This means that the surface pinning is *collective* similar to the collective pinning in the bulk [2]. But close to B_{c2} the VL distortion by surface pinning become essential, and near the surface the ordered VL transforms to the disordered vortex array, which we call *surface vortex glass*. Formation of the surface vortex glass is accompanied by the crossover from collective to individual pinning. This results in the growth of the critical current, i.e. in PE.

Experiments are performed on a series of millimeter-thick slabs of very pure Nb. Starting from electro-chemically polished samples, a controlled corrugation is introduced by ion-beam etching (IBE) the surfaces with a 1.5mA/cm^2 flux of 500eV-Ar^+ ions for 10–100 min. Given the sputter yield, 0.6 Nb atom per Ar^+, and the atomic spacing $c = 0.26$ nm, the average etching rate is of the order of 100 nm/min. From this stochastic process, one expects a roughness amplitude $\zeta^* \simeq (c\overline{\Delta z})^{1/2}$ and a white spectrum $S_\zeta(\mathbf{k}) = \int \mathbf{dr}\, e^{-i\mathbf{kr}} \langle \zeta(\mathbf{r} +$

$\mathbf{R})\zeta(\mathbf{R})\rangle_{\mathbf{R}} = c^3\overline{\Delta z}/\pi$ in the range $0 - c^{-1}$ of wave number k. In practice, the wave number cut-off $k_c < 1/c$ due crystal rearrangement associated with local heating; whence a reduction of ζ^* by a factor $k_c c \sim 10^{-1}$. This picture is confirmed by AFM-inspection, which shows a flat spectrum below $1\mu\mathrm{m}^{-1}$ and a power law dependence $S_\zeta(k) \sim 1/k$–$1/k^2$ above. The etched surfaces have a broad-band corrugation, in the range $k = 1$–$100\mu\mathrm{m}^{-1}$ covering the vortex reciprocal-lattice unit $Q = a_0^{-1} \simeq (50\mathrm{nm})^{-1}$, which is very effective for VL-pinning. Here $a_0 = \sqrt{\varphi_0/\pi B}$ is the radius of the vortex Wigner-Seitz cell (on the order of the intervortex spacing) and $\varphi_0 = h/2e$ is the flux quantum.

The pinning strength is deduced form the AC response. The AC surface impedance $Z(\omega) = -i\mu_0\omega\lambda_{AC}$ is determined by the effective penetration depth given by

$$\frac{1}{\lambda_{AC}} = \frac{1}{L_S} + \left(\frac{1}{\lambda_C^2} + i\omega\mu_0\sigma_f\right)^{1/2}; \quad L_S = \frac{l_S B}{\mu_0 \varepsilon} \quad . \tag{1}$$

Here σ_f is the flux-flow resistivity, $\varepsilon\varphi_0$ is the vortex-line tension (energy per unit length), and λ_C the Campbell penetration depth for bulk pinning. The surface pinning is taken into account by the length $L_S \sim 0.1$–100μm, which can simulate the effect of bulk pinning characterized by the Campbell depth λ_C. This expression was derived within the frame of the *two-mode electrodynamics* [11,12], which incorporates the surface pinning by introducing a phenomenological boundary condition,

$$\varepsilon\varphi_0\left(\frac{\mathbf{u}(0)}{l_S} + \frac{\partial\mathbf{u}(0)}{\partial z}\right) = 0 \ , \tag{2}$$

imposed on the average VL displacement $\mathbf{u}(z) = \overline{\mathbf{u}(\mathbf{r}, z)}$ at the surface of the sample, which occupies the semispace $z < 0$. Here l_S is a *slippage length* and the displacement $\mathbf{u}$ is averaged over the position vectors $\mathbf{r}$ in the xy plane. Physically this boundary condition presents the balance between the pinning force $-\varepsilon\varphi_0\mathbf{u}(0)/l_S$ and the line tension force $\varepsilon\varphi_0\partial\mathbf{u}(0)/\partial z$ due to the vortex bending.

Figure 1 shows the PE due to surface pinning. Data relate to sample #S2 with dimensions $25 \times 10.1 \times 0.87$ mm^3. The sample was annealed in ultra-high vacuum which gives a low residual resistivity $\rho_{\mathrm{n}} = 11$ nΩcm and $B_{\mathrm{c2}} = 0.29$ T at $4.2K$. This value is consistent with

earlier measurements within the anisotropy of Nb crystals ($B_{c2}(\theta) = 0.280$-0.295 at 4.2K) [13]. From the 90 min IBE exposure we estimate $\zeta^* \sim 5$ nm, in qualitative agreement with AFM measurement. Data points are obtained by fitting the penetration-depth spectra as shown in the inset of the figure. Metastability in the vortex number and/or arrangement is removed by feeding a large transient current ($I = 40$A) in the sample prior to measurement. The abrupt onset of the AC-flux penetration along the samples edges which are parallel to the field precludes quantitative analysis for $B \gtrsim 0.95 B_{c2}$; this difficulty can be overcome by working in oblique field (figure 1). More experimental details including the calibrating procedure can be found in Refs. [12]. Already present in pristine samples, the PE is strongly enhanced by IBE up to a factor of 3 at the maximum dose. This contrasts with conventional mechanical or chemical treatments which show ineffective in increasing the PE in our Nb samples. This distintive property of IBE emphasizes the importance of small-scale atomic corrugation for the surface pinning of vortex lines.

We separate quantitatively the bulk and surface contributions by relying on the full 1kHz–1MHz spectrum $\lambda_{AC}(f)$ [12]. From fits of $\lambda_{AC}(f)$ with Eq.(1) we deduce L_S, λ_C and σ_f. Remarkably enough, we always find $\lambda_C \gtrsim 10$m, meaning that the bulk pinning strength is negligible. In fact there is no difference in the spectra taken on both sides of the peak which are equally well described by Eq.(1). This confirms that surface pinning is most relevant for the vortex dynamics in our experiment. The oblique-field data are larger by a factor ~ 2; this general trend is due to surface-reinforcement of superconductivity in tilted fields. Similar data are observed at lower temperatures, with, however, larger $B_{pk} = 0.95 B_{c2}$ (1.8K) and a less pronounced PE.

Using the Abrikosov expression, $\mu_0 \varepsilon \simeq (B_{c2} - B)/2.32\kappa^2$ for $B \lesssim B_{c2}$, with $\kappa = 1.3$, and $B_{c2} = 0.29$T, we deduce from Eq.(1) the $l_S(B)$-data in Fig.2. By taking the bulk expression for ε, we disregard surface enhancement in oblique field and therefore overestimate the l_S^{-1} data in this geometry. The high-field plateaus $l_S = l_0$ above B_{pk} in Fig.2 are suggestive of an individual pinning, since in this case the slippage length is given by a typical curvature radius of the corrugated surface, which should not depend on the vortex density (magnetic

field). This interpretation is supported by the fact that the contact angle for VL at the surface $a_0/l_0 \simeq 0.1$, estimated from $l_0 \simeq 0.5\mu$m (normal field), agrees with the maximum tilt $\zeta^*/a_0 \sim 0.1$ deduced from surface corrugation. This suggests that the surface-pinning strength above B_{pk} is indeed limited by geometrical considerations. By contrast, the strong suppression of $1/l_S$ below B_{pk} (factor $\sim$10 in oblique field) reflects the *collective* regime of surface pinning, which was known earlier in rotating ^{3}He [14]. The transition is sharp unlike the continuous ones reported in Refs. [6,8]. Thus the experiment provides an evidence that PE is accompanied by the crossover from the collective to the individual surface pinning.

We start the theoretical analysis from calculation of the elastic response of the semi-infinite vortex lattice to the surface force presented by one Fourier component $\mathbf{f}(\mathbf{r}) = \mathbf{f}(\mathbf{k})e^{i\mathbf{kr}}$. Any surface force on a vortex should be balanced by the line-tension force: $\mathbf{f}(\mathbf{r}) = \varepsilon\varphi_0\partial\mathbf{u}/\partial z$. Thus the force produces the displacement field in the bulk, which is assumed to be transverse ($\mathbf{U}(\mathbf{k}) \perp \mathbf{k}$), since the VL is much more rigid with respect to the longitudinal force than to the transverse one. The equation of the elasticity theory is:

$$\left[C_{66}k^2 + C_{44}(\mathbf{k})k_z^2\right]\mathbf{U}(\mathbf{k}) = 0 \ , \tag{3}$$

where C_{66} is the shear modulus and

$$C_{44}(\mathbf{k}) = \frac{B^2}{\mu_0}\frac{1}{1+\lambda^2(k^2+k_z^2)} + \varepsilon B \tag{4}$$

is the tilt-modulus, which takes into account nonlocal effects due to long-range vortex-vortex interaction. The solution of equation (3) yields two values for $k_z^2 = -p^2$, which correspond to the *two modes* generated in the bulk. Usually $C_{66} \ll \varepsilon B \ll B^2/\mu_0$ and approximately

$$p_1^2 = \frac{(1+\lambda^2k^2)C_{66}}{B^2/\mu_0 + \varepsilon B\lambda^2k^2}k^2 \ , \ p_2^2 = \frac{B}{\mu_0\varepsilon\lambda^2} + k^2 \gg p_1^2 \ . \tag{5}$$

The solution is a superposition of two components, $U(x,z) = e^{ikx}\left(u_1e^{p_1z} + u_2e^{p_2z}\right)$, with the amplitudes u_1 and u_2 determined from the boundary conditions. The first one is given by the surface force: $f(\mathbf{k}) = \varepsilon\varphi_0(p_1u_1 + p_2u_2)$, and the second one is that the tangential magnetic field determined by the London equation, $\mathbf{h}(\mathbf{k}) = ik_zB\mathbf{U}(\mathbf{k})\left[1+\lambda^2(k^2+k_z^2)\right]^{-1}$, vanishes at

the sample border. Eventually one can find the linear response relation $f(\mathbf{k}) = C(k)U_0(\mathbf{k})$, which connects the force and the displacement $U(x,0) = U_0 e^{ikx}$ at the surface in the Fourier presentation, where $U_0 = u_1 + u_2$ and

$$C(k) \approx k\varphi_0 \sqrt{\frac{C_{66}}{\mu_0} \frac{(1+\lambda^2 k^2 \mu_0 \varepsilon/B)}{1+\lambda^2 k^2}} \ . \tag{6}$$

Most of the deformation energy is stored in the first long-wavelength mode.

The linear-response function allows to calculate the random displacements produced by the surface pinning. Considering that vortex cores end perpendicular to the local surface, the corrugation produces a force $f_m(\mathbf{r_i}) = -\varepsilon\varphi_0 \partial\zeta(\mathbf{r_i})/\partial \mathbf{x}_m$ applied to the end of the vortex line, where $\mathbf{r}_i = \mathbf{R_i} + \mathbf{U}_0$ is the 2D position vector of the vortex end. For small displacements $\mathbf{U}_0$, the balance of force yields the boundary condition

$$\varepsilon\varphi_0 \left[\frac{\partial \mathbf{U}_{0m}(\mathbf{R_i})}{\partial z} + \frac{\partial \zeta(\mathbf{R_i})}{\partial x_{\rm m}} \right] = 0 \quad . \tag{7}$$

In the Fourier presentation the random force is $\mathbf{f}(\mathbf{k}) = -i\mathbf{k}\varepsilon\varphi_0 \int d\mathbf{r}\, e^{-i\mathbf{kr}} \zeta(\mathbf{r})$. Since $C(k) \propto k$ at small k, the integral for the mean-square-root displacement is divergent at small k. But we can obtain a convergent integral for the mean-square-root shear deformation

$$\left\langle (\nabla \mathbf{U}_0)^2 \right\rangle = \left\langle (\partial U_{0x}/\partial y + \partial U_{0y}/\partial x)^2 \right\rangle$$
$$= \frac{\varepsilon^2 \varphi_0^2}{4\pi^2} \int \frac{\mathbf{k^2}\, \mathbf{dk}}{\mathbf{C(k)^2}} \sum_{\mathbf{Q}} \left(Q^2 - \frac{(\mathbf{k}\cdot\mathbf{Q})^2}{k^2} \right) S_\zeta(\mathbf{k}+\mathbf{Q}) \tag{8}$$

Here the integration over $\mathbf{k}$ is fulfilled over the Brillouin zone and $\mathbf{Q}$ is the reciprocal vortex-lattice vector. We shall approximate the surface corrugation spectrum as $S_\zeta(\mathbf{k}) = 2\pi\zeta^{*2} r_d^2 e^{-kr_d}$, where $\zeta^* = \sqrt{\langle \zeta(\mathbf{R})^2 \rangle_{\mathbf{R}}}$ is the amplitude of the surface roughness and r_d is the correlation length of the random pinning force, which cannot be much less than the coherence length ξ. In the collective regime $k \lesssim Q$, considering a broad corrugation spectrum ($r_d \ll a_0$), summation over $\mathbf{Q}$ can be replaced by integration, and we obtain

$$\left\langle (\nabla \mathbf{U}_0)^2 \right\rangle = \frac{\varepsilon^2 \varphi_0^2 a_0^2}{8\pi} \int_0^{2/a_0} \frac{k^3\, dk}{C(k)^2} \int_0^\infty S_\zeta(Q) Q^3\, dQ$$
$$\approx \frac{\varepsilon B}{C_{66}} \frac{3 r_d^2}{l_0^2} \ , \tag{9}$$

where $l_0 = r_d^2/\zeta^*$ is on the order of the geometric curvature radius. Here we have used the large k limit of Eq.(6), $C(k) \approx k\varphi_0(C_{66}\varepsilon/B)^{1/2}$, which is a good approximation when $\lambda \gg a_0$.

In the experiment the AC fields produce additional quasistatic displacements $\mathbf{u}(\mathbf{R}_i)$ superimposed on the static displacements induced by pinning. By differentiating Eq.(7) for small $\mathbf{u}$, we obtain the boundary condition:

$$\frac{\partial \mathbf{u}_{\rm m}(\mathbf{R}_i)}{\partial z} + \frac{\partial^2 \zeta(\mathbf{R}_i)}{\partial x_{\rm m} \partial x_{\rm n}}\, \mathbf{u}_{\rm n}(\mathbf{R}_i) = 0 \qquad . \tag{10}$$

In the Fourier presentation the uniform displacement ($\mathbf{k} = 0$) is coupled with the nonuniform displacements ($\mathbf{k} \neq 0$). Treating the latter by the perturbation theory we arrive at the the boundary condition Eq. (2) imposed on the averaged, i.e., uniform displacement with slippage length given by

$$\frac{1}{l_S} \simeq \frac{\varepsilon\varphi_0}{4\pi^2} \sum_{\mathbf{Q}} \int \mathbf{dk}\, |\mathbf{k}+\mathbf{Q}|^2 \left[Q^2 - \frac{(\mathbf{k}\cdot\mathbf{Q})^2}{k^2} \right] \times \frac{S_\zeta(\mathbf{k}+\mathbf{Q})}{C(k)} \quad . \tag{11}$$

Using the same approximation as in calculating $\langle (\nabla \mathbf{U}_0)^2 \rangle$ we receive for the inverse slippage length

$$\frac{1}{l_S} = \frac{\varepsilon\varphi_0 a_0^2}{8\pi} \int_0^{2/a_0} \frac{k dk}{C(k)} \int_0^\infty S_\zeta(Q) Q^5\, dQ \approx \sqrt{\frac{\varepsilon B}{C_{66}}} \frac{5! a_0}{2 l_0^2} \ . \tag{12}$$

Our derivation of the collective pinning strength $\propto 1/l_S$ was not based on the heuristic concept of Larkin-Ovchinnikov domain [2] usually used for the analysis of collective pinning. The domain size L_c is determined by the balance of the pinning energy and the elastic energy. The average energy density of pinning weakened by collective effects is $E_p \sim \varepsilon\varphi_0 u^2/a_0^2 l_0 \sqrt{N_c}$, where $N_c = L_c^2/a_0^2$ is the number of vortices in the Larkin-Ovchinnikov domain. In order to estimate the elastic energy one should know how far the shear deformation from surface disorder penetrates into the bulk. This length is not evident *apriori*, but *aposteriori*, from our analysis. Both experiment and theory show the importance of the short lengthscales, $k^{-1} \sim a_0$ for the surface pinning; as a consequence, the deformation penetration length,

$\sim 1/p_1 \sim \sqrt{\varepsilon\varphi_0/C_{66}}$ which corresponds to large k limit in Eq. (5), is finite. Then the elastic energy per unit area is $E_{el} \sim (C_{66}/p_1)(u^2/L_c^2) \sim \sqrt{C_{66}\varepsilon\varphi_0}u^2/L_c^2$. The condition $E_p \sim E_{el}$ yields $L_c \sim l_0 a_0\sqrt{C_{66}/\varepsilon\varphi_0}$ and since $l_S \sim l_0\sqrt{N_c} = l_0 L_c/a_0$ one obtains for l_S the value of the same order as in Eq. (12).

Let us apply the received expressions for the magnetic fields far from B_{c2}. In this case $\varepsilon \sim (\varphi_0/\mu_0\lambda^2)\ln(B_{c2}/B)$, $C_{66} \sim \varphi_0 B/\mu_0\lambda^2$ and according to Eq. (12) $l_S \propto \sqrt{B/\ln(B_{c2}/B)}$. Then the surface length $L_s \propto [B/\ln(B_{c2}/B)]^{3/2}$ grows with the magnetic field in qualitative agreement with the experiment (Fig. 1). This is a regime of collective pinning when $l_S > l_0$. At the same time since $r_d \ll a_0$ the vortex lattice shear deformation remains small according to Eq. (9). Close to B_{c2} $\varepsilon \sim (B_{c2} - B)/\mu_0\kappa^2$, $C_{66} \sim (B_{c2} - B)^2/\kappa^2$, and $r_d \sim a_0 \sim \xi$. Then from Eqs. (9) and (12) we receive that $\langle(\nabla \mathbf{U}_0)^2\rangle \approx (\xi^2/l_0^2)B_{c2}/(B_{c2} - B)$ and $l_S \approx (l_0^2/\xi)\sqrt{(B_{c2} - B)/B_{c2}}$. Thus l_S decreases when B approaches to B_{c2} and becomes smaller than l_0 for $B_{c2} - B < B_{c2}\xi^2/l_0^2$. This means that surface pinning ceases to be collective and the transition to the individual pinning occurs. At the same time, at $B_{c2} - B \sim B_{c2}\xi^2/l_0^2$, the deformation $\langle(\nabla \mathbf{U}_0)^2\rangle$ becomes of the order of unity, which means destruction of the crystalline order at the surface. The state without the crystalline order near the surface can be called *surface glass*. Thus the crossover from the collective to the individual pinning is accompanied by the crystal-glass transition at the surface.

Now let us check that this transition, or crossover, can explain PE. Despite the fact that $l_S \propto \sqrt{B_{c2} - B}$ decreases at B approaching to B_{c2}, according to Eq. (1) L_S continues to grow proportionally to $1/\sqrt{B_{c2} - B}$ whereas in the experiment (Fig. 1) $L_S(B)$ decreases close to the peak. However, the growth of the deformation $\langle(\nabla \mathbf{U}_0)^2\rangle$, which accompanies the decrease of l_S eventually invalidates the perturbative approach used above. Qualitatively this can be corrected by introducing the renormalized deformation-dependent shear modulus in the form $\tilde{C}_{66} = C_{66}(1 - \alpha\,\langle(\nabla \mathbf{U}_0)^2\rangle) \approx C_{66}(1 - B/B_{pk})$. Here the field B_{pk} corresponds to the crystal-glass transition, where $\tilde{C}_{66} = 0$, and α is an unknown numerical factor, which could be close to 0.1 as in the Lindemann criterion. Using renormalized modulus $\tilde{C}_{66}$ in place

of C_{66} in Eq. (12) we obtain that l_S as well L_S [see Eq. (1)] decrease inversely proportionally to $\sqrt{B_{pk} - B}$ in qualitative agreement with experiment (Figs. 1 and 2). On the right of the peak, where pinning is individual and the shear rigidity is absent, $l_S \sim l_0$ does not depend on the magnetic field B, while $L_S \propto 1/(B_{c2} - B)$ grows with B.

The close relation between PE and vanishing of the shear modulus of VL was suggested in the early studies of PE [1,2]. The new feature in our scenario is that the shear vortex elasticity vanishes only in some surface layer. The width $\sim 1/p_1 \propto 1/\sqrt{C_{66}}$ of this layer diverges if $C_{66} \to 0$ and finally surface disorder can contaminate the bulk of the sample. But this should happen for fields $B > B_{pk}$, since the peak field B_{pk} is determined by $\tilde{C}_{66}$. Our scenario agrees with recent STM imaging of the vortex array by Troyanovski *et al.* [15]. This experiment has revealed the disorder onset *on the surface* of 2H-$NbSe_2$ sample, coinciding with the onset of the peak effect. Troyanovski *et al.* related the disorder onset with the bulk pinning. In order to discriminate two scenarios it would be useful to supplement the STM probing of the vortex array at the surface by probing vortex arrangements in the bulk.

In conclusion, this experiment and the accompanying theoretical model provide a new plausible scenario for the peak effect. This is a comprehensive demonstration of a new situation: the order-disorder transition in a vortex lattice triggered by a weak surface disorder. Beside its experimental relevance, this new established mechanism offers an interesting paradigm for elastic systems at the upper critical dimension for disorder.

We thank F.R. Ladan and E. Lacaze for technical assistance. We acknowledge fruitful discussions with B. Horowitz, T. Natterman and T. Giamarchi. This work was funded by the French-Israel Keshet program and by the grant of the Israel Academy of Sciences and Humanities.

REFERENCES

[1] A.B. Pippard, Philos. Mag. **19**, 217 (1969).

[2] A.I. Larkin and Y.N. Ovchinnikov, J. Low Temp. Phys. **34**, 409 (1979).

[3] S.H. Autler, E.S. Rosenblum, and K.H. Goen, Phys. Rev. Lett. **9**, 489 (1962).

[4] P.H. Kes and C.C. Tsuei, Phys. Rev. Lett. **47**, 1930 (1981).

[5] Jing Shi, X.S. Ling, Ruixing Liang, D.A. Bonn, and W.H. Hardy, Phys. Rev. B **60**, R12593 (1999).

[6] Y. Paltiel, E. Zeldov, Y. Myasoedov, M.I. Rappaport, G. Jung, S. Bhattacharya, M. J. Higgins, Z.I. Xiao, E.Y. Andrei, P.L. Gammel, and D.J. Bishop, Phys. Rev. Lett. **85**, 3712 (2000).

[7] P.L. Gammel, U. Yaron, A.P. Ramirez, D.J. Bishop, A.M. Chang, R. Ruel, L.N. Pfeiffer, E. Bucher, G. D'Anna, D.A. Huse, K. Mortensen, M.R. Esklidsen, and P.H. Kes, Phys. Rev. Lett. **80**, 833 (1998).

[8] X.S. Ling, S.R. Park, B.A. McClain, S.M. Choi, D.C. Dender, and J.W. Lynn, Phys. Rev. Lett. **86**, 712 (2001).

[9] T. Giamarchi and P. Le Doussal, Phys. Rev. B **52**, 1242 (1995).

[10] T. Klein, L. Joumard, S. Blanchard, J. Marcus, R. Cubbit, T. Giamarchi, and P. Le Doussal, Nature **413**, 404 (2001).

[11] E.B. Sonin, A.K. Tangatsev, and K.B. Traito, Phys. Rev. B **46**, 5830 (1992).

[12] N. Lütke-Entrup, B. Plaçais, P. Mathieu, and Y. Simon, Phys. Rev. Lett.**79**, 2538 (1997); *ibid*, Physica B**255**, 75 (1998).

[13] S.J. Williamson, Phys. Rev. B **2**, 3545 (1970).

[14] M. Krusius, J.S. Korhonen, Y. Kondo, E.B. Sonin, Phys. Rev. B **47**, 15113 (1993).

[15] A.M. Troyanovski, M. van Hecke, N. Saha, J. Aarts, and P.H. Kes, Phys. Rev. Lett. **89**, 147006 (2002).

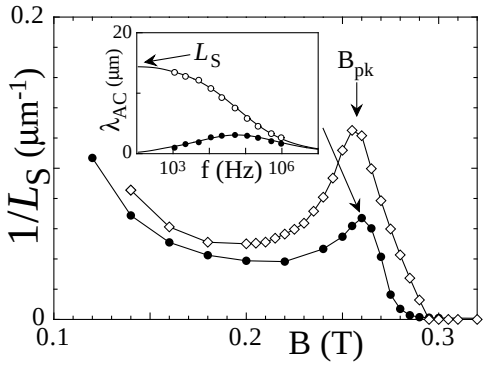

FIG. 1. Peak-effect in the elastic response $L_S^{-1}(B)$ of a surface-pinned vortex array. Diamonds and full circles correspond to oblique and perpendicular field orientations in sample #S2 at T=4.2K. Inset: the frequency dependence of the real and imaginary parts (open and full circles respectively) of the penetration depth $\lambda_{AC}(B, f)$ from which L_S is deduced. Solid lines are theoretical fit to Eq.(1) with $\lambda_C = \infty$, $\sigma_f^{-1} = 10$nOhm.cm and $L_S = 14.9\mu$m.

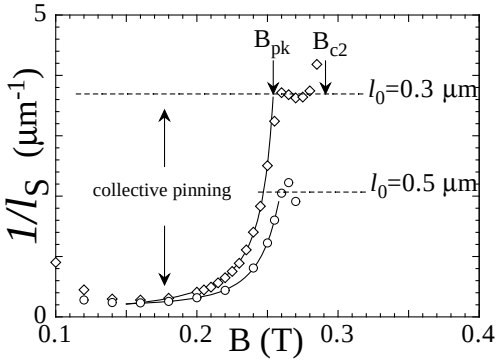

FIG. 2. The inverse of phenomenological slippage length $l_S(B)$ for a vortex array at a rough surface. It is deduced from the L_S data in Fig.1 according to the definition $l_S = L_S\mu_0\varepsilon/B$ in Eq.(1). The effect of vortex interactions in the collective-pinning regime below B_{pk} is visible as a strong reduction in $1/l_S(B)$. Solid lines are power-law fits to the data at the transition.